

SMALL-ANGLE X-RAY SCATTERING FROM TURNIP  
YELLOW MOSAIC VIRUS\*

by

PAUL SCHMIDT\*\*, PAUL KAESBERG\*\*\* AND W. W. BEEMAN

*Department of Physics, University of Wisconsin, Madison,  
Wisconsin (U.S.A.)*

## INTRODUCTION

An earlier communication<sup>1</sup> from this laboratory discussed the small-angle X-ray scattering from solutions of three spherical plant viruses: southern bean mosaic virus, tobacco necrosis virus, and tomato bushy stunt virus. In the present contribution similar methods are applied to turnip yellow mosaic virus and the associated protein particle. The virus is of particular interest because of the nucleic acid-free protein particle which is produced, along with the multiplication of the virus, in the diseased host.

MARKHAM<sup>2</sup> has given many of the physical parameters of these particles. The virus has a molecular weight of  $5 \cdot 10^6$  and a dry partial specific volume of 0.666 ml/g. The corresponding values for the protein particle are  $3 \cdot 10^6$  and 0.740 ml/g. Electron microscope and X-ray crystallographic<sup>3</sup> evidence indicates that both particles are near spherical. Assuming this shape, a radius of the hydrated sphere may be calculated from the measured diffusion constants. MARKHAM obtained a radius of about 138 Å for the virus particle and 141 Å for the protein. The difference is not beyond experimental error.

Further evidence of the near identity of size, shape and surface structure of the two particles is furnished by the ease with which they form mixed crystals and their very similar serological properties.

Based on the above data, MARKHAM suggested the protein parts of the two particles had similar spatial configurations, either a spherical shell or a sponge-like structure. In the virus the holes are filled with nucleic acid and in the protein with water. The X-ray evidence to be presented confirms the size and shape given by MARKHAM and strongly supports the hollow sphere structure.

## EXPERIMENTAL

The experimental equipment and procedures are similar to those described in reference 1.  $\text{CuK}_\alpha$  radiation from a rotating anode X-ray tube is collimated by two

\* Research supported in part by the Office of Naval Research and in part by the Wisconsin Alumni Research Foundation.

\*\* National Science Foundation Fellow, now with the Department of Physics, University of Missouri, Columbia, Missouri.

\*\*\* Department of Biometry and Physics, University of Wisconsin.

fixed slits. Scattered radiation from the sample passes through a third and fourth slit mounted on an arm which can be rotated about an axis through the scattering sample. All four slits are identical and successive slits are 50 cm apart. The sample is placed midway between the second and third slits. Just beyond the fourth slit is a Ross double filter for spectral isolation of the  $\text{CuK}_\alpha$  line and a Geiger counter for intensity measurements.

A mixture of protein and virus as crystals under ammonium sulphate was kindly given to us by Dr. R. MARKHAM of Cambridge University. These were dissolved and separated by differential centrifugation according to the method described by MARKHAM. The virus and protein were obtained in essentially pure water solutions of weight concentration 13% and about 0.9% respectively. Scattering curves were run with the solutions in thin-walled Pyrex tubes of roughly rectangular cross section about 1 mm thick and 2 mm wide.

The fundamental equation in the interpretation of the experimental data is the scattering function for a sphere of uniform electron density.

$$\Phi^2(ha) = \left[ \frac{3(\sin ha - ha \cos ha)}{(ha)^3} \right]^2$$

In this equation  $a$  is the sphere radius and  $h = 4\pi/\lambda \sin \theta/2$ , where  $\lambda$  is the X-ray wavelength and  $\theta$  the scattering angle. This function has a pronounced central maximum, which can be approximated by a gaussian, and a series of much less intense subsidiary maxima and minima. In the central region the gaussian approximation is given by

$$\Phi^2(hR) = \exp \left[ -\frac{1}{3} (hR)^2 \right]$$

As has been shown by GUINIER<sup>4</sup> this is a good approximation, in the central region, to the scattering function of a particle of any shape.  $R$  is the radius of gyration of the particle. For a uniform sphere  $R^2 = \frac{3}{5} a^2$ . Our experimental curves include the central region (where the gaussian approximation may be used to determine the radius of gyration and thus the sphere radius) and extend through the third subsidiary maxima. Here, in the peak region, we use the known positions of the maxima and minima of the exact scattering function to evaluate the sphere radius.

However, both the given scattering functions assume perfect collimation of the incident and scattered rays. Real collimating apertures admit a range of angles about the nominal setting and in particular the slits used in this experiment introduce smearing effects which must be taken into account. In the central region (and for two runs through the first subsidiary maximum) we used slits 10 mm high and 0.15 mm wide. In the peak region slits were 10 mm by 0.5 mm.

It can be shown<sup>5</sup> that for particles of the size being measured the narrower slits are well approximated by slits of negligible width and infinite height. With the 0.5 mm slits an additional slit width correction must be made. This affects, however, only the positions of the first subsidiary minimum and maximum.

The scattering function for slits of negligible width and infinite height is given by<sup>6</sup>

$$F(ha) = \int_0^\infty \Phi^2 \left( \sqrt{(ha)^2 + Z^2} \right) dZ$$

where  $\Phi^2$  is the perfect collimation scattering function. This expression has been numeric-

ally integrated for uniform spheres by DEXTER AND ANDEREGG<sup>5</sup> and by SCHMIDT<sup>7</sup>. The slits are found to move the maxima and minima to somewhat smaller values of the argument  $ha$ , and of course, to fill in the minima, at which with perfect collimation the scattered intensity is zero. In Table I we give the arguments of the first three minima and maxima.

TABLE I

ARGUMENTS OF THE MINIMA AND MAXIMA OF THE SCATTERING FUNCTION FOR UNIFORM SPHERES WITH PERFECT COLLIMATION AND WITH SLITS OF NEGLIGIBLE WIDTH AND INFINITE HEIGHT

|          | <i>Perfect collimation</i> | <i>Slit smeared</i> |
|----------|----------------------------|---------------------|
| 1st Min. | $ha = 4.49$                | 4.34                |
| 1st Max. | 5.80                       | 5.3†                |
| 2nd Min. | 7.72                       | 7.5                 |
| 2nd Max. | 9.10                       | 8.6                 |
| 3rd Min. | 10.90                      | 10.7                |
| 3rd Max. | 12.32                      | 11.8                |

An additional correction for slit width is necessary with the 0.5 mm slits. We have calculated this and find that the argument at the first minimum is 4.55, and at the first maximum 5.27, corrected for both slit height and width. The positions of the higher maxima and minima are not appreciably affected by the width correction.

The experimental data are treated in the following way. From the experimental curves one obtains the angles at which various minima and maxima occur. Knowing the slit-corrected values of  $ha$  at which these extrema occur, one may solve for the sphere radius. All the experimentally measured extrema should give the same sphere radius. A failure to do so means that the particle is not a sphere of uniform electron density or that there are experimental inadequacies in the measurement of the scattering. As will be seen, both possibilities appear to have been realized.

In the central region it is customary to plot the logarithm of the scattered intensity versus the square of the scattering angle. The slope of the resulting straight line furnishes the radius of gyration. Here also the use of slits necessitates corrections. These have been discussed by GUINIER AND FOURNET<sup>6</sup>. In addition, the gaussian is an approximation to the exact scattering function which is best at the smallest angles. At the angle of half maximum intensity the gaussian lies about 4% above the correct value. At the smallest angle at which we could take data the scattering was about 80% of the central maximum, and in order to have enough points to establish with some certainty the shape of the scattering curve we have used data out to about one-third of the central maximum. For the particles under investigation, this is the angular range from about two to four thousandths of a radian.

Simultaneous corrections for slit height and the failure of the gaussian approximation are made as follows. The exact spherical scattering function, corrected for slits of negligible width and infinite height, is plotted (log intensity versus angle squared) in the angular range from about eight-tenths to one-third of the central (or zero angle) intensity. The plot is not quite a straight line because of the failure of the gaussian approximation. The best straight line is then fitted to this plot by a least squares adjustment. It is found that the apparent radius of gyration from this line must be multiplied by the factor 0.93 in order to give the correct radius of gyration of the sphere.

About half of this correction is to be attributed to the effects of the slits and half to the failure of the gaussian approximation at the larger angles.

A similar procedure can now be applied to the experimental curves. A best straight line through experimental data in the above angular region is determined by a least squares adjustment and the apparent radius of gyration multiplied by 0.93 to give a correct experimental radius of gyration for the particle being measured.

The experimental radii about to be discussed have been subjected to the corrections, appropriate to the region of the curve from which they are derived.

## RESULTS

### *The virus particle*

In Fig. 1 is shown an experimental curve through the third maximum taken with 0.5 mm slits and in Fig. 2 the central region through the first maximum taken with 0.15 slits. In both cases the solid line is the theoretical curve for a uniform sphere of 141 Å radius corrected for slits of negligible width and infinite height. For the narrower slits the agreement is excellent except at the smallest angles where the very appreciable deviation of the experimental points from the theoretical curve is due to interparticle

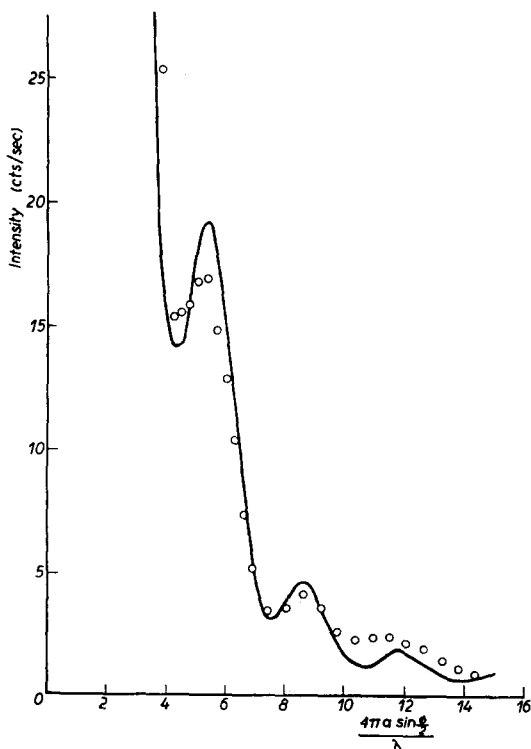


Fig. 1. Peak region scattering from a 13% virus solution, slit width 0.5 mm. The experimental points are shown by circles. The solid line is the theoretical scattering curve for a uniform sphere of 141 Å radius corrected for slits of infinite height and negligible width.

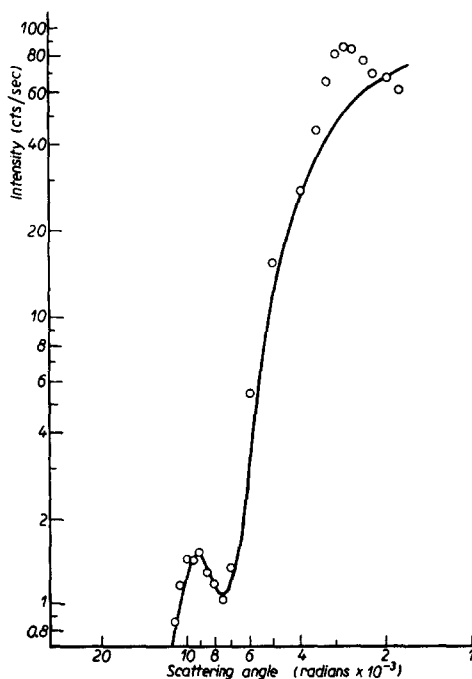


Fig. 2. Central region scattering and first subsidiary maximum from a 13% virus solution, slit width 0.15 mm. The experimental points are shown by circles. The solid line is the theoretical scattering curve for a uniform sphere of 141 Å radius corrected for slits of infinite height and negligible width.

interference effects in the fairly concentrated solution used. These effects will be discussed later.

With the wider slits the effect of slit width in smearing out the extrema is visible and near the third maximum the scattered intensity seems too high. This might be due to an incorrect background subtraction. Backgrounds were determined by placing pure water in the sample holder and amounted to about one count per second over most of the angular range measured. It was necessary to stop taking data when scattered intensities approached this value as they did at the third maximum. Similar difficulties which could be ascribed to an error in background were met when taking data in the central region with very dilute samples and with counting rates of the order of magnitude of the background.

In Table II we give the sphere radii which are obtained from the measured positions of the various maxima and minima.

TABLE II  
RADIUS OF THE VIRUS PARTICLE AS DETERMINED FROM THE ANGULAR POSITIONS OF  
THE FIRST THREE MINIMA AND MAXIMA. SLIT COLLIMATION WAS USED

| Virus sphere radius |                |                |
|---------------------|----------------|----------------|
|                     | <i>Minimum</i> | <i>Maximum</i> |
| 1                   | 138 A          | 140 A          |
| 2                   | 138            | 142            |
| 3                   | 146            | 147            |

An average of 141 A, giving lesser weight to the doubtful values from the third minimum and maximum, was decided upon and used in drawing the theoretical curves of Figs. 1 and 2.

As a check on the slit corrections and on a recently completed scattering chamber using pinhole collimators and an annular ring pick-up of the scattered radiation, an additional run in the peak region was made with the new equipment. The apparatus will be described in detail in another journal. The results are given in Table III.

TABLE III  
RADIUS OF THE VIRUS PARTICLE AS DETERMINED FROM THE ANGULAR POSITIONS OF  
THE FIRST THREE MAXIMA AND MINIMA. PINHOLE COLLIMATION WAS USED

| Virus sphere radius |                |                |
|---------------------|----------------|----------------|
|                     | <i>Minimum</i> | <i>Maximum</i> |
| 1                   | 138 A          | 140 A          |
| 2                   | 141            | 140            |
| 3                   | 147            | 144            |

Of course, no slit height corrections were used in obtaining these radii, although it was necessary to apply a correction for the finite size of the pinholes and annular ring. This correction is analogous to that for slit width. The agreement with the previous results is highly satisfactory. Again there is a tendency for the third minimum and

maximum to give a rather larger radius. Fig. 3 illustrates some of the data taken with the new scattering chamber.

In addition to the measurements in the peak region, radii were determined from the central region by the method already described. Here one must use solutions more dilute than the 13% weight concentration used in the peak region. As has been mentioned, this is necessitated by the inter-particle interference effects which increase with concentration and which are so noticeable in Fig. 2 at the smaller angles. Radii of gyration measurements were made at a series of concentrations between 3.2% and 0.32%. The lowest concentrations had to be measured at counting rates of the same order of magnitude as the background and did not give results in good agreement with those obtained at the higher concentrations. The results are given in Table IV.

TABLE IV

EXPERIMENTAL RADII OF GYRATION AS A FUNCTION OF CONCENTRATION FOR THE VIRUS PARTICLE

| Concentration | Radius of gyration | Sphere radius |
|---------------|--------------------|---------------|
| 3.2%          | 112 Å              | 145 Å         |
| 1.6           | 107                | 138           |
| 0.95          | 107                | 138           |
| 0.63          | 103                | 133           |
| 0.32          | 99                 | 128           |

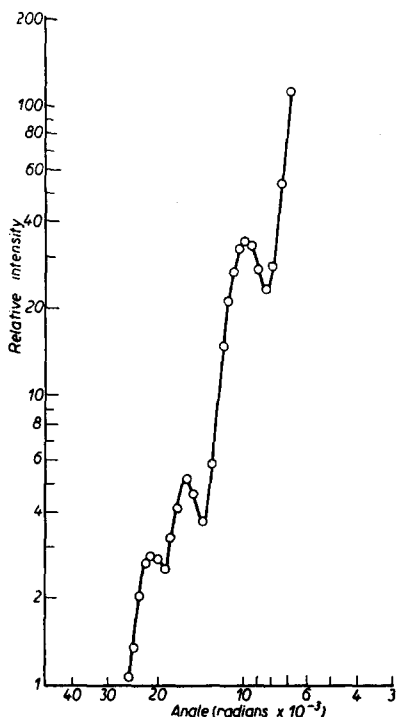


Fig. 3. Peak region scattering from a 13% virus solution taken with the pinhole collimation apparatus with 0.5 mm pinholes. The curve is drawn through the experimental points.

If the background was underestimated by 0.2 or 0.3 cts/sec, the sphere radii would be in much better agreement at about 139 Å.

In summary, then, the several measurements indicate a sphere radius for the virus particle of about 140 Å. We believe this should not be in error by more than 2 or 3%. If one gives negligible weight to measurements taken at low counting rates, the internal consistency of the results is appreciably better than this.

#### *The protein particle*

For several reasons the data on the protein particle are not as complete as on the virus particle. Smaller amounts of protein were available. It could not be prepared conveniently at a concentration greater than about 0.9% and all data were taken at this concentration. In addition, at a given concentration, the scattering from the protein is considerably smaller than from the virus because of the lower electron density.

In Figs. 4 and 5 are shown protein scattering curves for the central and peak region. The radius of gyration from the central region is 125 Å. If the particle were a uniform sphere, this would imply a sphere radius of 163 Å. The measured positions of maxima and minima determine the sphere radii given in Table V, again assuming a uniform sphere.

In reducing the data the same corrections have been used for slit shape and for deviation from the GUINIER approximation as were applied to the virus data. This is not strictly permissible, since the corrections depend upon the scattering function and, as we shall see, the protein particle is not a uniform sphere. However, slit corrections are not available for the hollow sphere. Because of the general similarity of the hollow sphere and uniform sphere scattering functions, the error introduced by this procedure is expected to be small.

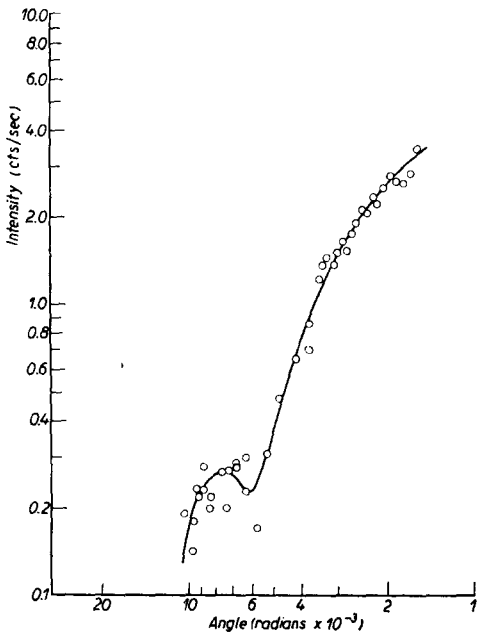


Fig. 4. Central region scattering and first subsidiary maximum from a 0.93 % solution of the protein particle, slit width 0.15 mm. The curve is drawn through the experimental points.

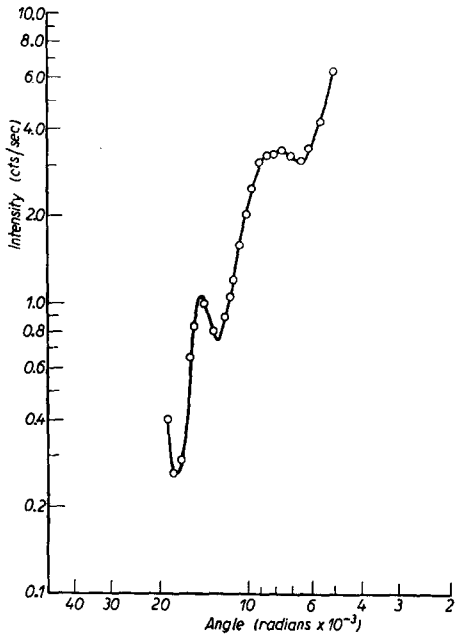


Fig. 5. Peak region scattering from a 0.93 % solution of the protein particle, slit width 0.5 mm. The curve is drawn through the experimental points.

TABLE V  
THE RADIUS OF THE PROTEIN PARTICLE AS DETERMINED FROM THE POSITIONS OF SEVERAL SCATTERING MAXIMA AND MINIMA. THE PARTICLE IS ASSUMED TO BE A UNIFORM SPHERE

| Protein sphere radius |         |         |
|-----------------------|---------|---------|
|                       | Minimum | Maximum |
| 1                     | 172 A   | 168 A   |
| 2                     | 145     | 148     |
| 3                     | 149     |         |

To return to the data themselves, one notices first the very poor agreement among the various measured radii and, second, that the average radius (157 A) is appreciably greater than the 140 A determined for the virus, although chemical evidence indicates they should be about the same size. All this suggests that a different model should be

tried in interpreting the protein data. The scattering function for a hollow sphere has been calculated by LEONARD<sup>8</sup>. It exhibits an infinite sequence of subsidiary maxima and minima, somewhat displaced in position and different in intensity from those of the uniform sphere.

In Table VI we give the outer sphere radii determined from a hollow sphere model with a ratio  $h$  of inner radius to outer radius of 0.75. The radius of gyration of 125 Å interpreted on this model implies an outer radius of 141 Å, in agreement with the 141 Å which is the average of the values in Table VI.

TABLE VI  
OUTER RADII OF PROTEIN PARTICLE CONSIDERED AS A HOLLOW SPHERE ( $h = 0.75$ )

|   | Outer radius (hollow sphere) |                |
|---|------------------------------|----------------|
|   | <i>Minimum</i>               | <i>Maximum</i> |
| 1 | 143 Å                        | 144 Å          |
| 2 | 133                          | 141            |
| 3 | 146                          |                |

Only slightly less satisfactory internal consistency is achieved assuming  $h = 0.6$ . However, the outer radius then calculates to 151 Å in poor agreement with the virus radius.

Within the experimental error one may say that both the virus and protein particle have a radius of about 140 Å.

Further evidence that the protein particle must be considered a hollow sphere is obtained from the intensity of the first subsidiary maximum compared to the central maximum. We determined the intensity of the first subsidiary maximum to be about 1.4% of the central maximum for the virus particle and 6.5% for the protein particle. Calculations for slits of infinite height show that this ratio should be 1.6% for uniform spheres in agreement with observation for the virus particle. With perfect collimation, this ratio is 0.74% for uniform spheres and 4.0% for a hollow sphere with  $h = 0.75$ . Thus, if we assume that slits affect the hollow sphere curve about the same as they do that of a uniform sphere, all the data are in satisfactory agreement with the assumption that the virus is a uniform sphere and the protein a hollow sphere (filled with water when in solution) with  $h = 0.75$ . Both particles have an outer radius of 140 Å. Comparisons of intensity between the central and peak regions are probably reliable to 10 or 15%.

## DISCUSSION

For the purpose of further discussion, the assignment of size and shape just made will be used.

As in the case of the three viruses already discussed<sup>1</sup>, the present small-angle scattering measurements furnish strong evidence for the internal hydration of TYMV. From the molecular weight and partial specific volume one calculates that the dry virus particle, if spherical and compact, would have a radius of 110 Å. Electron micrographs<sup>2</sup> indicate a radius of about 115 Å for both the dry protein and dry virus particle. The separations of nearest neighbours in the dry crystal<sup>3</sup> give maximum dry radii of



119 Å and 115 Å for the protein and virus, respectively. As pointed out by MARKHAM<sup>2</sup>, these data imply that the protein particle maintains its hollow sphere structure even when dry, since the molecular weight and partial specific volume would give a radius of about 96 Å to a compact sphere.

Since the X-rays see only that volume having an electron density different from water, the 140 Å radius measured is the extent of the amino acid structure itself and should not include external hydration. This is in rather too good agreement with MARKHAM's hydrodynamic radii quoted in the introduction, since these latter should include external hydration. However, the probable errors in the two measurements will easily permit one or two molecular layers of external water.

BERNAL AND CARLISLE<sup>3</sup> measured effective radii (half the nearest neighbour separation) in wet single crystals of 157 Å for the protein and 153 Å for the virus. These are appreciably greater than MARKHAM's radii. Both particles crystallize in the diamond lattice. In explanation of the low coordination number and large nearest neighbour separation, BERNAL AND CARLISLE<sup>3</sup> suggested that the particles may be somewhat tetrahedral in shape. This may very well be the case, as slight deviations from the spherical shape would probably not be detectable in the small-angle scattering curve. The alternative to assuming a tetrahedral shape, with nearest neighbours almost in contact at the corners, is to believe that the rigidity of the wet crystal can be maintained even though nearest neighbours are separated by 30 Å of water. The existence of internal hydration has, of course, somewhat relaxed this dilemma. Without internal hydration, the separation of the surfaces of nearest neighbours (assumed spherical) would be 76 Å.

The actual internal hydrations calculated from the molecular weight, partial specific volume and the hydrated sphere radius of 140 Å are 0.71 g of water per gram of dry virus for the virus particle and 0.6 g of water per gram of dry protein for the protein particle. The latter refers only to the hydration of the spherical shell and excludes the water presumably contained in the center. The hydration of the spherical shell is quite sensitive to the ratio of inner to outer radius. At  $h = 0.86$  the hydration becomes zero.

It is necessary to consider in greater detail the separate hydrations of the protein and nucleic acid in the virus particle. We have considered the virus particle to be a sphere of constant electron density. Actually, the electron densities of dry protein and nucleic acid are quite different. Taking water as unity they are, respectively, 1.29 and 1.62. We can get a hydrated virus particle of uniform electron density only by assigning different hydrations to its two components. With  $h = 0.75$  the required hydrations are 0.88 g of water per gram of nucleic acid and 0.59 g of water per g of protein. These give the correct total hydration to the virus and the 0.59 is in satisfactory agreement with the 0.6 determined for the shell hydration of the protein particle. These calculations assume that the protein and virus particles contain the same amount of protein. This was established by MARKHAM.

A final check on the consistency of the data may be obtained by comparing the ratio of the forward scattering per molecule for the two particles. This may be calculated knowing the volume and electron density of the particle. Experimentally, the virus scattering per molecule in the forward direction was about 4.1 times that of the protein. One calculates a ratio of 4.3. The agreement is within experimental error. This is not a check on the assignment of hydration since the forward scattering depends only on the dry molecular volume of the scatterer and its electron density.

In Fig. 6 we present the central region of the virus scattering curve at a series of fairly high concentrations. The two higher concentrations exhibit very clearly the maximum which is introduced when interparticle interference effects become large. FOURNET<sup>9</sup> has recently given an expression for the X-ray scattering by a fluid in terms of the density and interparticle potential rather than the pair distribution function. The new formulation, which is based upon the Born-Green theory of liquids, is especially convenient for a discussion of interparticle interference effects in solutions of large molecules,

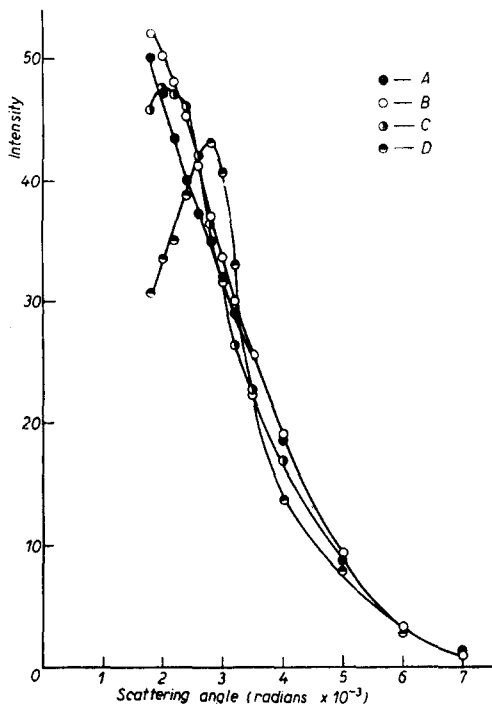


Fig. 6. Interparticle interference effects on the central region scattering from concentrated virus solutions. The ordinates are adjusted so that if scattering were proportional to concentration at every angle, the curves would coincide. The curves are drawn through the experimental points. Slit widths were 0.15 mm. Concentrations of 1.6, 3.2, 6.3 and 12.8% are shown by curves A, B, C and D, respectively.

since the solute may be considered a gas and the solvent a homogeneous medium which makes no contribution to the scattering except through its effect on the interparticle potential. The concentration or effective density may conveniently be varied through a considerable range. In principle, a sufficiently complete set of X-ray scattering curves would permit the determination of the interparticle potential. DOTY AND STEINER<sup>10</sup> have made an interesting application of the theory to the scattering of light by serum albumin solutions.

The present data allow only some crude deductions. FOURNET<sup>9</sup> considers the case of a gas of hard spheres. As the density is increased the central or zero angle scattering maximum is depressed until finally a maximum appears at a finite angle as in Fig. 6. This first occurs at a value of the parameter  $8v_0\epsilon/v_1$  of slightly less than two. Here  $\epsilon$  is a constant very close to unity,  $v_0$  is the volume of the molecule and  $v_1$  is the reciprocal of the number of molecules per unit volume.

We observe that with the virus particle, an interparticle interference maximum is found at a weight concentration of 6.3%. The slits tend to smear out maxima and minima and we may assume, for the purpose of calculation, that with perfect collimation, a maximum would be observed at 5% concentration.

This determines  $v_1$  and putting the parameter equal to two we find  $v_0 = 4.15 \cdot 10^7 \text{ \AA}^3$ . This is almost four times the volume of a sphere of radius 140 \AA. Thus the virus particles do not behave as a gas of hard spheres without interaction except upon contact. Their effective collision diameter is some 1.6 times their actual diameter. Presumably this is to be explained in terms of repulsive forces between the molecules.

One may also compare the observed angle of the interparticle interference maximum with that expected on the hard sphere model. The observed angle is too small by almost a factor of two, again indicating a large effective diameter.

## ACKNOWLEDGEMENTS

We wish to express our thanks to Dr. ROY MARKHAM of Cambridge University who generously supplied the TYMV, and to Mr. ROBERT V. RICE and Professor MARK STAHMANN of the Biochemistry Department of the University of Wisconsin who kindly undertook the task of separating the two components.

## SUMMARY

The small-angle X-ray scattering has been measured from solutions of turnip yellow mosaic virus and the associated protein. The data indicate that both particles are near spherical and about 140 Å in radius. The virus is of approximately uniform electron density. The protein is a water-filled spherical shell with a ratio of inner to outer radius of 0.75. The 140 Å quoted represents the radius of the protein structure excluding external hydration. Thus both particles have large internal hydrations. A reasonable assignment of hydration to the protein and nucleic acid fractions of the virus particle is possible, which gives the particle an approximately uniform electron density.

## RÉSUMÉ

Les auteurs ont mesuré la dispersion des rayons X sous angle faible par des solutions du virus de la mosaïque jaune du navet et de la protéine qui lui est associée. Les résultats montrent que les deux particules sont sensiblement sphériques et ont un rayon d'environ 140 Å. La densité électronique du virus est à peu près uniforme. La protéine se présente comme une enveloppe sphérique remplie d'eau, le rapport entre les rayons internes et externes étant de 0.75. La valeur de 140 Å indiquée plus haut se rapporte au rayon de la protéine, et ne tient pas compte de l'hydratation externe. Ainsi les deux particules ont des hydrations internes importantes. Il est que de la particule du virus, de telle façon que la densité électronique de la particule soit approximativement uniforme.

## ZUSAMMENFASSUNG

Die Kleinwinkel-Röntgenstrahlstreuung von Lösungen des Rüben-Gelben Mosaic-Virus und dem verbundenen Protein wurde gemessen. Die Daten zeigen, dass beide Teilchen kugelförmig sind und einen Radius von ungefähr 140 Å besitzen. Das Virus ist von ungefähr einheitlicher Elektronendichte. Das Protein ist eine mit Wasser gefüllte kugliche Schale und das Verhältnis vom inneren zum äusseren Radius beträgt 0.75. Die 140 Å stellen den Radius des Proteins ohne Berücksichtigung seiner äusseren Hydratationshülle dar. Daher haben beide Teilchen eine grosse innere Hydratation. Es ist möglich dem Protein und den Nucleinsäurefraktionen des Virusteilchens Hydratationswasser zuzuordnen und man erhält so eine ungefähr einheitliche Elektronendichte für die Teilchen.

## REFERENCES

- <sup>1</sup> B. R. LEONARD, Jr., J. W. ANDEREGG, S. SHULMAN, PAUL KAESBERG AND W. W. BEEMAN, *Biochim. Biophys. Acta*, 12 (1953) 499.
- <sup>2</sup> R. MARKHAM, *Discussions Faraday Society*, 11 (1951) 221.
- <sup>3</sup> J. D. BERNAL AND C. H. CARLISLE, *Nature*, 162 (1948) 139.
- <sup>4</sup> A. GUINIER, *Ann. Phys.*, 12 (1939) 16.
- <sup>5</sup> J. W. ANDEREGG, Thesis, Univ. of Wis. (1952).
- <sup>6</sup> A. GUINIER AND G. FOURNET, *J. Phys. et Rad.*, 8 (1947) 345.
- <sup>7</sup> P. W. SCHMIDT, Thesis, Univ. of Wis. (1953).
- <sup>8</sup> B. R. LEONARD, Jr., Thesis, Univ. of Wis. (1951).
- <sup>9</sup> G. FOURNET, *Acta Crystallographica*, 4 (1951) 293.
- <sup>10</sup> P. DOTY AND R. F. STEINER, *J. Chem. Phys.*, 20 (1952) 85.

Received November 7th, 1953